# A Continuum/Discontinuum Micro Plane Damage Model for Concrete

**S. A. Sadrnejad[1] and M. Labibzadeh[2]**

Department of Civil Engineering, K.N. Toosi University of Technology

Tehran, Iran

[1]Email: sadrnejad@srttu.edu, sadrnejad@hotmail.com

[2]Email: mojtabalabibzadeh@yahoo.com

***Abstract:*** *Analysis and prediction of structural response to static or dynamic loading requires prediction of concrete response tovariable load histories. The constitutive equations for the mechanical behavior of concrete capable of seeing damage effects or crack growth procedure under loading/unloading/reloading was developed upon micro-plane framework. The proposed damage formulation has been built on the basis of five fundamental types of stress/strain combinations, which essentially may occur on any of micro-planes. Model verification under different loading/unloading/reloading stress/strain paths has been examined. The proposed model is capable of presenting pre-failure history of stress/strain progress on different predefined sampling planes through material. Many of mechanical behavior aspects happen during plasticity such as induced anisotropy, rotation of principal stress/strain axes, localization of stress/strain, and even failure mechanism are predicted upon a simple rational way and can be presented.*

## 1.Introduction

The fundamental characteristics of concrete behavior are established through experimental testing of plain concrete specimens subjected to specific, relatively simple load histories. Continuum mechanics provides a framework for developing an analytical model that describe these fundamental characteristics. Experimental data provide additional information for refinement and calibration of the analytical model.

The continuous models in turn consist of two large groups: macroscopic models in the context of damage and plasticity theory or combination of both and meso-scopic models such as micro-plane or multi-laminate models. The macroscopic models concern with the definition of relation between stress and strain tensors (structural scale) and the meso-scopic models deals with the same object but in the different way. The latter capture this goal by assigning of the relation between the stress and strain components of the different planes with prescribed orientations 'called micro or multi planes'. Finally the microscopic models concern with the discrete particle models consisting of convex polygons that are able to withstand a limited cohesion (granular scale). A description of contacts of particles as well as a bond formulation between them could lead to forces induced by particle movements. These forces are inserted into the equations of motion, which are solved numerically based on the discrete element methodology.

In this research, we pay our attention for the micro or multi plane models, which nowadays are developed as powerful tools for numerical simulation of the geo and geo-like materials. Nevertheless, these models have been formulated and used by many researchers in the recent years; it seems to be necessary to review these models in the new deeper mathematical way to prevent any mistakes, which unfortunately have been made by the users of these models.

### 1.1From slip planes to micro planes

The basic idea, namely that of the constitutive material behavior as a relation between strain and stress tensors can be

"assembled" from the behavior of material on the planes with different orientations within the material such as slip planes, micro cracks, particle contacts, etc., might be traced back to the failure envelopes of Mohr (1900) and the "slip theory of plasticity" of G.I. Taylor (1938) who was the first that implemented this mentioned theory for modeling the behavior of polycrystalline metals. Taylor's idea was formulated in detail by Batdorf and Budiansky (1949). This theory was soon recognized as the most realistic constitutive model for plastic-hardening metals. It was refined in a number of subsequent works (e.g. Lin and Ito 1965, 1966, Kröner 1961, Budianski and Wu 1962, Hill, 1965, 1966, Rice, 1970). It was used in arguments about the physical origin of strain hardening, and was shown to allow easy modeling of anisotropy as well as the vertex effects for loading increment to the side of a radial path in stress space. All the formulations considered that only the inelastic shear strains (`slips'), with no inelastic normal strain, were taking place on what is now called the 'micro-planes'. The theory was also adapted to anisotropic rocks and soils under the name "multi laminate model" (Zienkiewicz and Pande 1977, Pande and Sharma 1981, 1982; Pande and Xiong 1982). It is interesting to note that in these works there is a common assumption that the planes of plastic slip in the material (in those studies called the `slip-planes' and here in this article called the `micro-planes') to be constrained statically to the stress (`macro-stress') tensor (i.e., the stress vector on each 'micro-plane' was the projection of). The elastic strain was not included on the slip planes but was added to the inelastic strain tensor on the continuum level (macro-level). The static constraint formulation was extensively used under the name of slip theory for metals or multi-laminate theory for anisotropic rocks until the first application of this theory by Bazant

and Gambarova in 1984 and Bazant in 1984, for continuum damage mechanics and cohesive-frictional materials, which for the first time its name changed from slip theory or multi-laminate theory to micro-plane theory. Bazant and coworkers have been interested in this domain of research and tried to simulate the strain-softening of geo-materials with such a theory which was not of interest in the aforementioned studies. After a short time, they concluded that under the assumption of the static constraint, a strain-softening constitutive law for the micro-plane makes the material unstable even if is prescribed. They suggested that it could be preferable if in replace of static constraint, the kinetic constraint is used. In the kinetic constraint approach, the strain tensor instead of stress tensor is projected on the planes.

## 2.Constraint Approach: Equilibrium and Compatibility

As it is mentioned in the previous section, before 1984, the early multi-plane models (called slip-planes theory or multi-laminate models) developed based on the static constraint formulation. Furthermore it was said that after 1984, Bazant and Gambarova and also Bazant and his assistants informed that to prevent instability of numerical simulation of post-peak behavior of cohesive-frictional materials it is necessary to use kinetic constraint formulation instead of static one. In this research, we will first focus on the superimposition method, which used in the static constraint formulation in the past and it will be shown that this formulation was not correct and then the reason of shortcomings of this approach will be argue.

Before 1984, in all the multi-plane models

such as slip-planes or multi-laminate models, first the macro-stress tensor was projected on the micro-planes and then by introducing on-plane constitutive laws, the micro-strain components were calculated and finally the macro-strain tensor was identified by superimposition of on-plane micro-strain components upon any of sampling plane transformation matrix obtained through direction cosines of sampling points on the surface of a unit sphere:

$$\int_{\Omega} f(x, y, z)d\Omega = 4\pi \sum_{p} W_p f(x_p, y_p, z_p) \quad (1)$$

Now consider the stress tensor in the macro-level state in the center of the unit sphere as always is used in the micro-plane models. Then, we are going to project this tensor on the planes, which are tangent on the surface of the sphere in the prescribed points. The number and position of these points are determined depending on the numerical integration formulation which elected for doing integration of an arbitrary function over the surface of the unit sphere. It is worth noting that the origin of the initiation and propagation of the all multi-plane models including micro-plane or multi-laminate models are as this mathematical numerical formulation used for integration. Here, we use a precise formulation of 26 integration points for this job. In the table 1, direction cosines and weights of the integration points and in figure 1, their positions on the surface of the unit sphere are shown.

If we project the stress tensor on the surface of the sphere, then we have:

$$\sigma_N = N_{ij}\sigma_{ij} \qquad , N_{ij} = n_i n_j$$
$$\sigma_M = M_{ij}\sigma_{ij} \qquad , M_{ij} = (m_i n_j + m_j n_i)/2$$
$$\sigma_L = L_{ij}\sigma_{ij} \qquad , L_{ij} = (l_i n_j + l_j n_i)/2$$
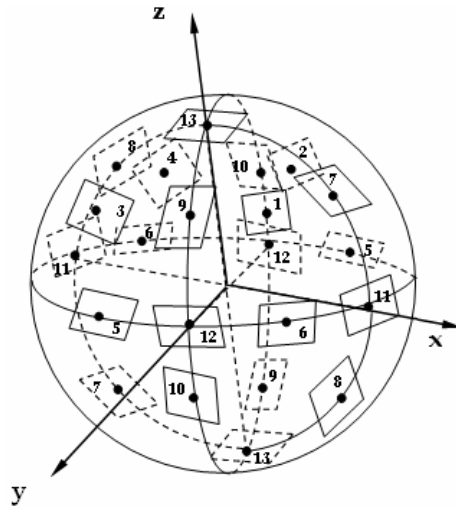
$$(2)$$



**Fig.1** Position of integration points on the unit sphere' surface

**Table 1** definition of micro-planes

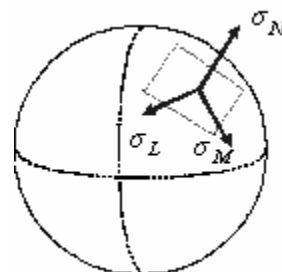| Direction cosines of integration points | | | Weights |
|---|---|---|---|
| $l_i$ | $m_i$ | $n_i$ | $W_i$ |
| $\sqrt{1/3}$ | $\sqrt{1/3}$ | $\sqrt{1/3}$ | 27/840 |
| $\sqrt{1/3}$ | $-\sqrt{1/3}$ | $\sqrt{1/3}$ | 27/840 |
| $-\sqrt{1/3}$ | $\sqrt{1/3}$ | $\sqrt{1/3}$ | 27/840 |
| $-\sqrt{1/3}$ | $-\sqrt{1/3}$ | $\sqrt{1/3}$ | 27/840 |
| $\sqrt{1/2}$ | $\sqrt{1/2}$ | 0.0 | 32/840 |
| $-\sqrt{1/2}$ | $\sqrt{1/2}$ | 0.0 | 32/840 |
| $\sqrt{1/2}$ | 0.0 | $\sqrt{1/2}$ | 32/840 |
| $-\sqrt{1/2}$ | 0.0 | $\sqrt{1/2}$ | 32/840 |
| 0.0 | $-\sqrt{1/2}$ | $\sqrt{1/2}$ | 32/840 |
| 0.0 | $+\sqrt{1/2}$ | $\sqrt{1/2}$ | 32/840 |
| 1.0 | 0.0 | 0.0 | 40/840 |
| 0.0 | 1.0 | 0.0 | 40/840 |
| 0.0 | 0.0 | 1.0 | 40/840 |



**Fig.2** Projection of stress tensor on the surface of unit sphere

In which $n_i$, $i=1,2,3$ are the direction cosines of the unit vector normal to the plane and $m_i$, $l_i$, $i=1,2,3$ are the direction cosines of two orthogonal unit vectors tangential to the plane.

For convenience of calculations, one of the unit vectors tangential to the plane is considered to be horizontal (parallel to *x-y* plane). For instance, the projection of the stress tensor on the plane number 1, results in:

$$\sigma_N = \frac{1}{3}\left(\sigma_x + \sigma_y + \sigma_z\right) + \frac{2}{3}\left(\tau_{xy} + \tau_{yz} + \tau_{zx}\right)$$

$$\sigma_M = \frac{1}{\sqrt{6}}\left(-\sigma_x + \sigma_y + \tau_{yz} - \tau_{zx}\right)$$

$$\sigma_L = \frac{1}{\sqrt{18}}\left(\sigma_x + \sigma_y - 2\sigma_z + 2\tau_{xy} - \tau_{yz} - \tau_{zx}\right)$$

(3)

Now, we try to obtain the original stress tensor from its projections on the micro-planes. To do so, it is first necessary to transfer every stress vector on the micro-plane from local coordinate to the global coordinate system and then we can add them up according to their weightings. Obviously, the result must be equal to numerical integration of the on-plane stress tensor. This numerical integration is a very crucial step in the construction of any micro-plane model. To transfer every micro-stress vector to the macro state the following transition matrix can be written:

$$T_p = \begin{bmatrix} N_{11} & M_{11} & L_{11} \\ N_{22} & M_{22} & L_{22} \\ N_{33} & M_{33} & L_{33} \\ N_{12} & M_{12} & L_{12} \\ N_{23} & M_{23} & L_{23} \\ N_{13} & M_{13} & L_{13} \end{bmatrix}_p$$

(4)

Subscript *p* denotes any specified micro-plane. So we can write:

$$\hat{\sigma}_p = T_p.\overline{\sigma} = T_p.\sigma : N_p$$

(5)

$$\sigma : N_p = \begin{bmatrix} n_1 & n_2 & n_3 \\ m_1 & m_2 & m_3 \\ l_1 & l_2 & l_3 \end{bmatrix} \begin{bmatrix} \sigma_x & \tau_{xy} & \tau_{xz} \\ \tau_{xy} & \sigma_y & \tau_{yz} \\ \tau_{xz} & \tau_{yz} & \sigma_z \end{bmatrix} \begin{bmatrix} n_1 \\ n_2 \\ n_3 \end{bmatrix}$$

(6)

For example, by transforming the micro-stress vector of the plane 1 to the macro level, we reach to the following six components vector:

$$\hat{\sigma}_1 = \frac{1}{6} \begin{Bmatrix} 2\left(\sigma_x + \tau_{xy} + \tau_{xz}\right) \\ 2\left(\sigma_y + \tau_{xy} + \tau_{yz}\right) \\ 2\left(\sigma_z + \tau_{zy} + \tau_{xz}\right) \\ \sigma_x + \sigma_y + 2\tau_{xy} + \tau_{yz} + \tau_{xz} \\ \sigma_y + \sigma_z + \tau_{xy} + 2\tau_{yz} + \tau_{xz} \\ \sigma_x + \sigma_z + \tau_{xy} + \tau_{yz} + 2\tau_{xz} \end{Bmatrix}$$

(7)

Summing up the transformed six component vectors according of their weighting functions:

$$\sum_{p=1}^{26} W_p \hat{\sigma}_P = \frac{1}{3}\left\{ \sigma_x \quad \sigma_y \quad \sigma_z \quad \tau_{xy} \quad \tau_{yz} \quad \tau_{zx} \right\}^T$$

(8)

Subscript *p* denotes any specified micro-plane.

As a general rule for the numerical integration of an arbitrary function *f(x,y,z)* over the surface of unit sphere, we can use the following 26 sampling point equations as follows:

$$\int_\Omega f(x, y, z)d\Omega = 4\pi \sum_{p=1}^{26} W_p f\left(x_p, y_p, z_p\right)$$

(9)

Comparing equation (8) and (9) we can write:

$$\int_{\Omega} \mathbf{T}.\boldsymbol{\sigma} : N d\Omega = \int_{\Omega} \hat{\boldsymbol{\sigma}} d\Omega =$$

$$4\pi \sum_{p=1}^{26} W_p \hat{\sigma}_p = \frac{4\pi}{3} \{ \sigma_x \quad \sigma_y \quad \sigma_z \quad \tau_{xy} \quad \tau_{yz} \quad \tau_{zx} \}^T$$

(10)

So, to obtain the original stress tensor we can write the following equation:

$$\sigma_{ij} = \frac{3}{4\pi} \int_{\Omega} (\sigma_N.N_{ij} + \sigma_M.M_{ij} + \sigma_L.L_{ij}) d\Omega$$

(11)

$$\sigma_{ij} = 3 \sum_{p=1}^{26} 6 \sum_{p=1}^{13} W_p (\sigma_N.N_{ij} + \sigma_M.M_{ij} + \sigma_L.L_{ij})$$

(12)

This comparison shows that the pre-multiplier in equation (12) and (1) for superimposition is not the same so it is not correct.

Furthermore, it is worth noting that in the static constraint approach, the equilibrium of the forces in a point are satisfied automatically because of the projection of the stress tensor on the planes, but the compatibility condition of strain tensor is met only in particular cases. In other words, the micro-strain components acting on the planes may not be always as the projection of the strain tensor, because the way of the superimposition of micro-strain components which are used in the static constraint approach (relation (1)) does not guarantee to be the same as the summation of the projections of macro-strain tensor obtained on every plane.

### 2.1 Kinetic constraint approach: equilibrium no, compatibility yes!

In 1984, Bazant and Gambarova suggested

that instead of projecting on-plane stress tensor, the strain tensor must be projected. Considering the previous argument, in this approach, static constraint has been replaced by kinetic constraint, however, the problem is still not solved because the compatibility is satisfied but equilibrium condition is not met. Although Bazant and his assistants tried to enforce the static equilibrium by application of the principle of virtual work; at the end they realized that the micro-stress components would not equal to the projection of macro-stress tensor. However, we note that the application of principle of virtual work is equivalent to establish the static equilibrium that latter itself equal to such a condition that micro-stress components on each plane are as the projection of macro-stress tensor. In fact, on the other words, the static equilibrium condition is not satisfied if and only if the micro-stress components that computed on the micro-planes are as the projections of the macro-stress tensor. So, regarding to the above rational argument and according to the investigations done by the authors, it is concluded that the formulation which Bazant and coworkers named it as principle of virtual work, basically is the only valid superimposition formula which was formerly derived by the authors and could not be the same as the application of usual virtual work (see relation 13, which derived by Bazant and compare it with relation 12).

$$\sigma_{ij} = \frac{3}{2\pi} \int_{\Omega} s_{ij} d\Omega \approx 6 \sum_{\mu=1}^{N_m} w_\mu s_{ij}^{(\mu)}, s_{ij} = \sigma_N N_{ij} + \sigma_L L_{ij} + \sigma_M M_{ij}$$

(13)

Furthermore it is worth noting that, equation (12) that has been derived based on the 26 integration point technique, is completely accurate but the equation (13) is fairly accurate.

## 2.2 Double Constraint Approach

To satisfy both of static equilibrium and compatibility conditions, we have considered a new method as projecting the stress tensor on the micro-planes as described earlier in this article. Then, we derived the strain tensor in terms of the stress tensor based on a well-capable constitutive relation in an ordinary three-dimensional coordinate system. In the second case, the derived strain tensor was projected or transformed on the micro-planes. So, in this stage, by comparing the components of stress and strain on the micro-planes we must be able to define the equal microscopic constitutive relations in such a way that both of the stress and strain components on each micro-plane are as the projections of the corresponding stress and strain tensors. This situation, in fact, is the double constraint formulation in which the equilibrium of forces and compatibility of displacements in every integration points are satisfied one by one.

## 3. Detachment of Behavior to Devitoric and Volumetric Parts

In order to attain to the double constraint aspect, after analogy of the projections of stress and strain tensors on the micro-planes obtained in the manner that was explained in the previous section, it was certain that it is necessary to separate the behavior of material into two distinct parts as deviatoric and volumetric. So if we discrete the strain tensor as the volumetric and deviatory parts firstly and then project each of them on the micro-planes separately, we may try to obtain the deviatoric part of the modules matrix from the behaviors which are taking place on the micro-planes and the volumetric one which is not affected by the direction characteristics and essentially is isotropic, obtained in the

ordinary coordinate system and summed up to the deviatoric part at the end of each step of loading. Therefore, we can write:

$$D_{ijkl} = \frac{3}{4\pi} \int_{\Omega} \left[ \left( \frac{E}{1+v} \right) \left[ \left( N_{ij} - \frac{\delta_{ij}}{3} \right) \left( N_{kl} - \frac{\delta_{kl}}{3} \right) + M_{ij} M_{kl} + L_{ij} L_{kl} \right] d\Omega$$

$$+ \frac{E}{1-2v} \frac{\delta_{kl}}{3} \delta_{ij} \tag{14}$$

## 4. Anistropy Damage Model

Total deviatory part of constitutive matrices is computed from superposition of its counterparts on the micro-planes that such counterparts in turn, are calculated based on the damages occurred on each plane depending on its specific loading conditions. This damage is evaluated according to the five separate damage functions; each of them belongs to the particular loading states. This five loading conditions are as:

-*hydrostatic compression,*
-*hydrostatic extension,*
-*pure shear,*
-*shear + compression,*
-*shear + extension.*

On each micro-plane at each time of loading history, there exists one specific loading situation that it may be in one of the five mentioned basic loading conditions. For every five mood, a specific damage function according to the authoritative laboratory test results available in the literature is assigned. Then, for each state of on plane loading, one of the five introduced damage functions will be computed with respect to the history of micro-stress and strain components.

### 4.1 Model Parameters

In this formulation we consider just two basic material parameters for ease as elasticity and Poisson's coefficients.
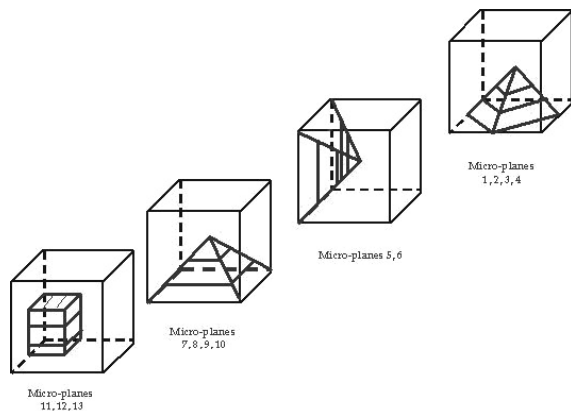
*International Journal of Civil Engineerng. Vol. 4 , No. 4, December 2006*

**301**

**Fig.3** Positions of the micro-planes in a cubic

### 4.2 Correlation Studies

To establish the validity of the proposed concrete material model, correlation studies of analytical results with experimental evidence from the stress-strain response of concrete specimens under different loading conditions are presented in the following.

**Uniaxial Compression (UC) test**

As can be seen in the figure 5, there is a good agreement between the results that were fulfilled by the proposed model and experimental evidences. The material parameters used in the above analysis are as: *E=25000MPa, v=0.20*.

In the figure 6, the volumetric changes of the concrete specimen under uniaxial compressive loading have been compared

with the experimental observations experienced by Kupfer and his co-workers in 1969. Obviously, there exists an excellent coincidence between analytical and laboratory data. To show more confidence on the capability of the micro-planes during uniaxial compression test, in the figure 7, the variation of micro-stress normal and tangential component values are represented verses the total axial compressive stress.

As can be seen from figure 7, during the application of the uniaxial compressive load on the x-axis, the micro-plane number 11 (see figure 1) is under just the compressive stress whereas the micro- planes number 9,10,12,13 which geometrically are located normal to the load direction on the unit sphere are only under the tensile stress. Compressive stress accompanied with shear affect the other remaining planes. It is interesting to note that during increase of the uniaxial compressive load, the compressive and shear stress components acting on the micro-planes number 1 to 8 increase together with more rise of shear stress at first, but near to the peak stress ($f_c^t$) the compressive stress decreases suddenly.

Figure 8 shows the growth of the damage function values of different micro-planes during uniaxial compression test of concrete obtained with the proposed model. As it can be well observed from this figure, damage evolutes faster on the micro-planes number 9,10,12,13 on the unit sphere than the other planes. On plane no. 11; there exists only a normal compressive load (mode I) by which no damages could be occurred on it. On the micro-planes number 5,6,7,8 there is a shear combined with the normal compressive load (mode IV) causes damages less than the micro-planes 1,2,3,4 on which there exists a same mode of loading (mode III). This is because of the fact that on the micro-planes number 1, 2, 3 and 4 the magnitude of the compressive stress component is less than the same component value on the micro-planes number 5 to 8 (see figure 7), so damage growths faster. Finally, on the micro-planes number 9,10,12,13 there exist only normal tension loading (mode II), causes the damage growths faster than the all other planes. This is introduced from proposed model that in the uniaxial compression test, the damages or cracks can be appeared first on the micro-
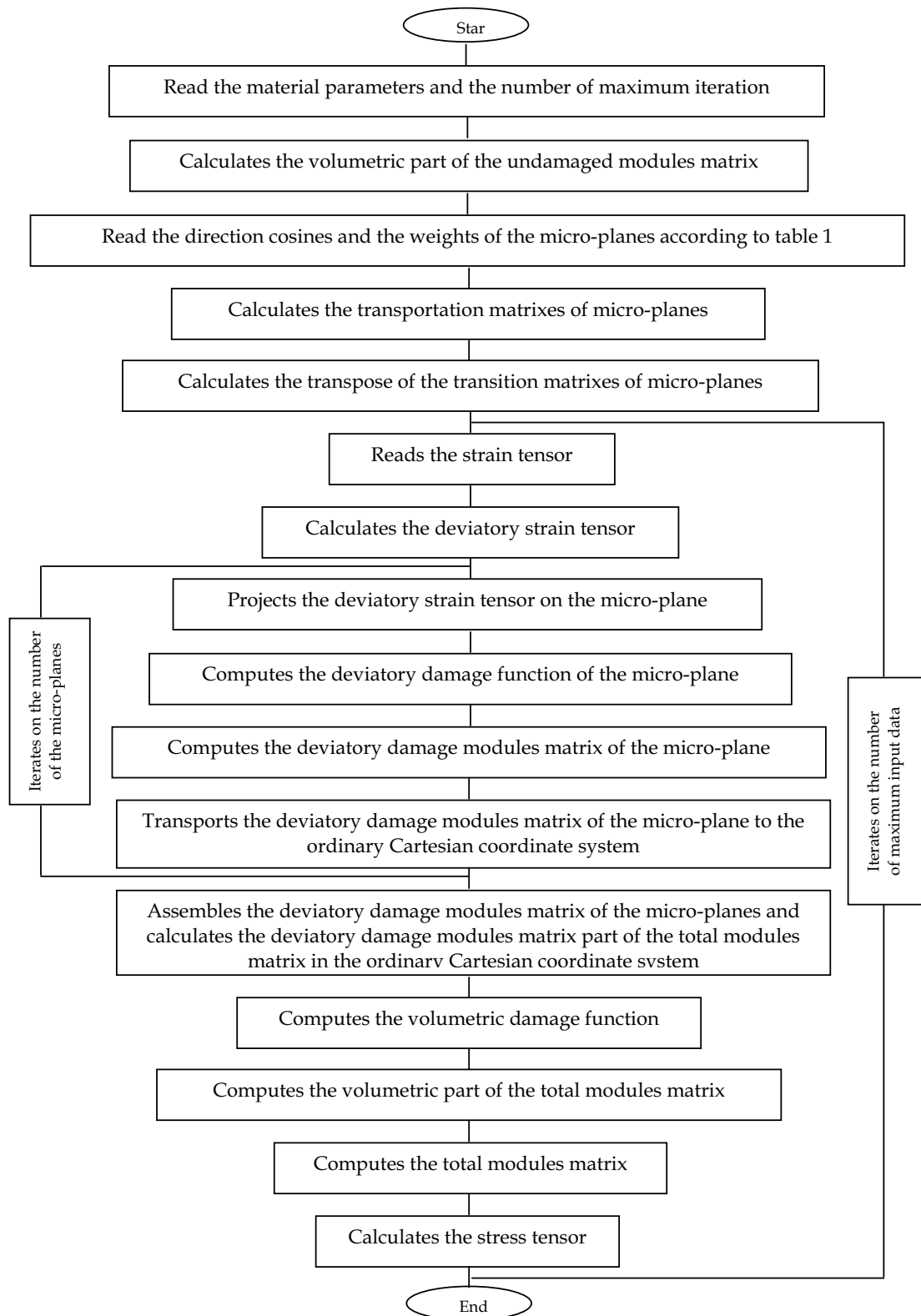
```
                           ( Star )

  Read the material parameters and the number of maximum iteration

      Calculates the volumetric part of the undamaged modules matrix

  Read the direction cosines and the weights of the micro-planes according to table 1

        Calculates the transportation matrixes of micro-planes

      Calculates the transpose of the transition matrixes of micro-planes

                    Reads the strain tensor

              Calculates the deviatory strain tensor

          Projects the deviatory strain tensor on the micro-plane

        Computes the deviatory damage function of the micro-plane

      Computes the deviatory damage modules matrix of the micro-plane

    Transports the deviatory damage modules matrix of the micro-plane to the
                  ordinary Cartesian coordinate system

    Assembles the deviatory damage modules matrix of the micro-planes and
    calculates the deviatory damage modules matrix part of the total modules
              matrix in the ordinary Cartesian coordinate system

                Computes the volumetric damage function

          Computes the volumetric part of the total modules matrix

                  Computes the total modules matrix

                    Calculates the stress tensor

                           ( End )
```

Iterates on the number of the micro-planes

Iterates on the number of maximum input data

**Fig.4** Operation sequence of the proposed micro-plane damage model developed in the VISUAL FORTRAN computer language

**Axial stress (MPa)**



$f_c' = 27MPa$

■   **Kupfer .et. al., 1969**

▲   **Kupfer .et. al., 1969**

**Lateral strain (mm/mm)**          **Axial strain (mm/mm)**

**uniaxial compression test of concrete obtained with proposed micro-plane damage model**
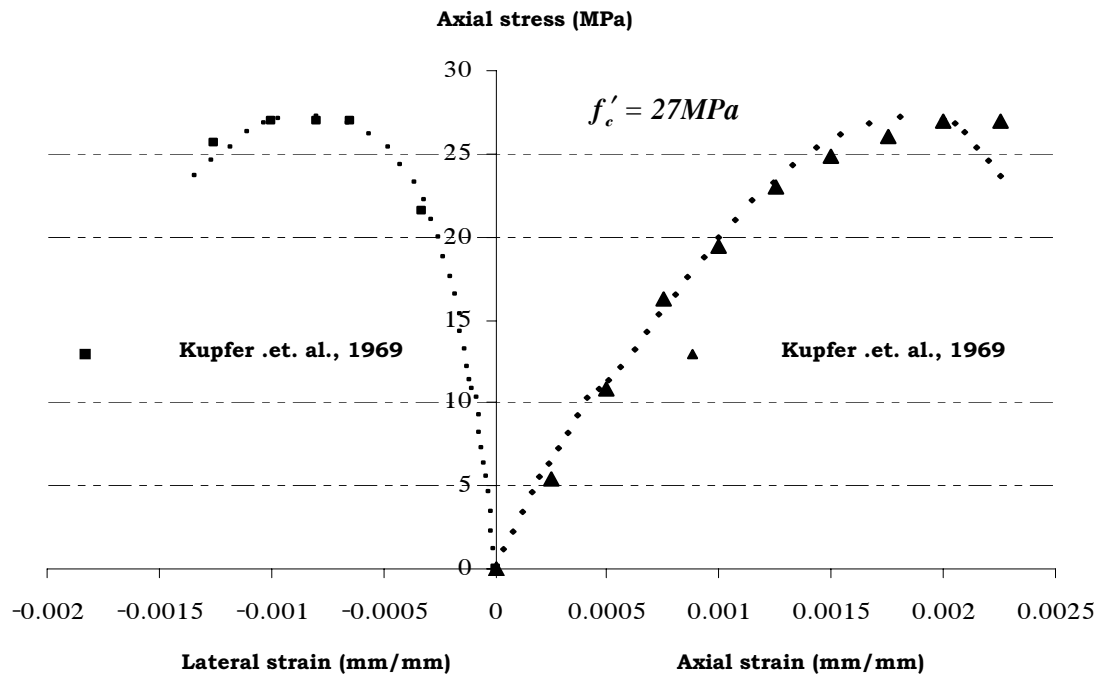
**Fig.5** Axial and lateral strains versus axial stress in uniaxial compression test of concrete obtained with proposed micro-plane damage model

**Axial compressive stress (MPa)**



$f_c' = 27MPa$

▲   **Kupfer .et. al., 1969**

**Contraction**          ⟵          ⟶          **Dilation**

**Volumetric strain (mm/mm)**
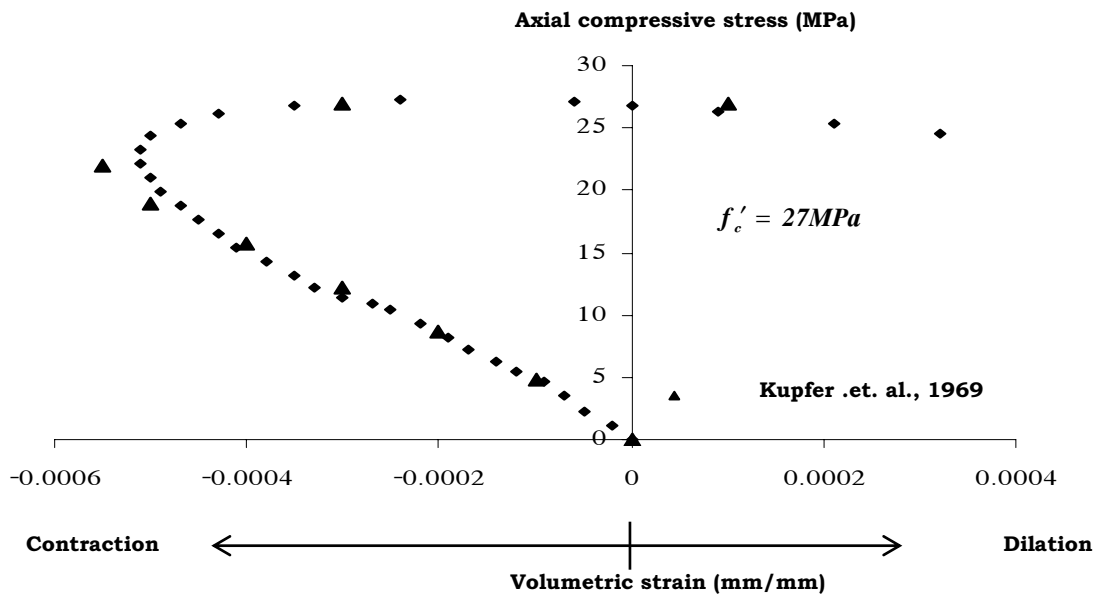
**Fig.6** Volumetric behavior of concrete under uniaxial compressive loading
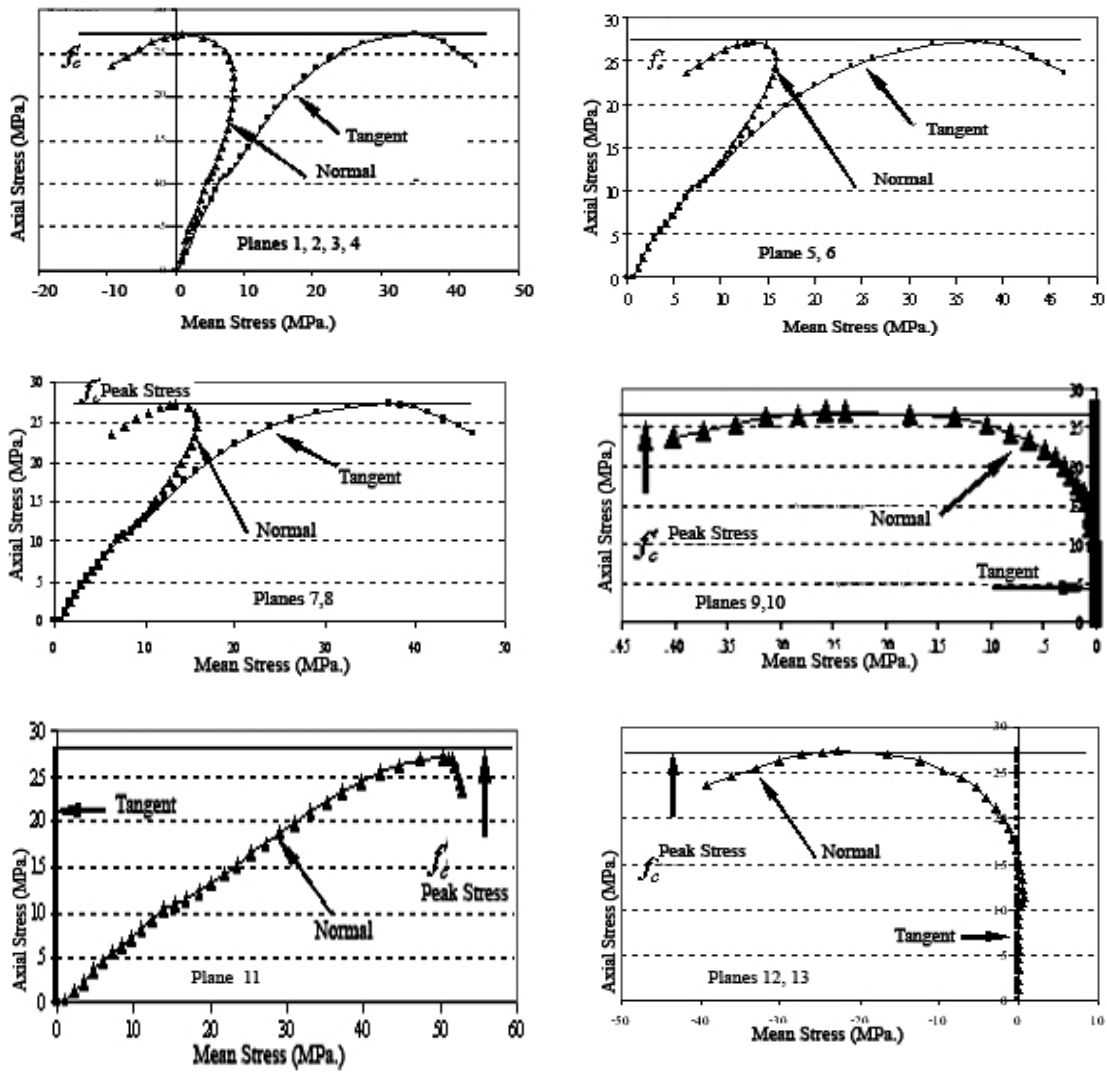
**Fig.7** Variation of micro-stress component values during uniaxial compression test
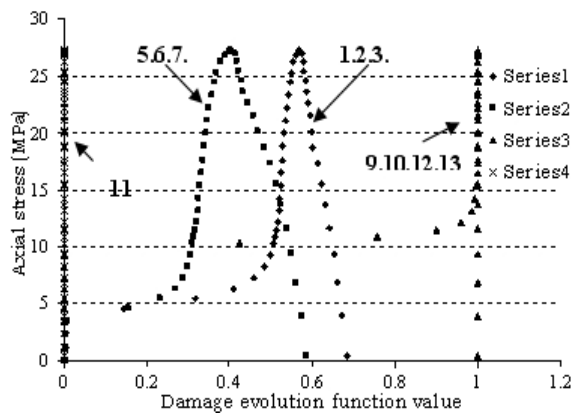


**Fig.8** Comparison of the damage evolution functions on the various micro-planes during the axial compressive loading
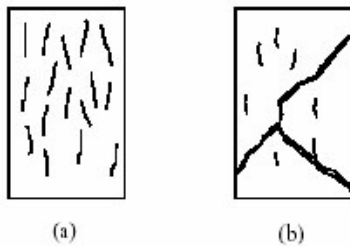
**Fig.9** Typical failure patterns of cylinders in uniaxial compression test with
a) low frictional b) high frictional restraint

planes number 9,10,12,13 and then on the micro-planes number 1, 2, 3 and 4. This can be so observed in the real situation of the laboratory on the cylindrical concrete specimen. If there is no friction restraint between the surfaces of the loading top/bottom plates and the specimen, the cracks will be appeared differently on the positions of the micro-planes number 9,10,12,13 of the proposed model. Else if the damages on the micro-planes number 1, 2, 3 and 4 will be greater and cracks will be initiated first on these planes. This phenomenon is depicted in the figure 9.

**Conventional Triaxial Compression (CTC) test**

In this test, at first the hydrostatic pressure is applied to the specimen to a certain level and then the axial compression is increased while the lateral or confining pressure held constant. So in this test, up to the certain level of hydrostatic compression there must be no any shear forces on the micro-planes. This can be seen in figure 10 that shows the evolution of the micro-stress components on the different micro-planes during CTC test.

In figure 11, the axial stress-strain curves of cylindrical concrete specimen under two different Uniaxial Compression (UC) test and Conventional Triaxial Compression (CTC) test obtained with proposed micro-

plane damage model have been compared. As it is observed from this result, the application of initial confining pressure of about %30 increases compression strength by( $0.3 \times f_c^t$ ), although, it can be improved approximately up to ( $1.4 \times f_c^t$ ).

As a result, the effect of lateral confining pressures on the compressive cylindrical strength of concrete specimens simulated by proposed model has been compared with experimental data of Ansari and Li (1998) in figure 12.

**Conventional Triaxial Extension (CTE) test**

To clarify the integrity of the proposed model in various loading conditions, this test is also considered. In this test, at first, the hydrostatic pressure is applied to the specimen to a certain level, but after that, the axial compression is decreased while the lateral pressure is held constant.

The stress component permutation during the CTE test on the specimen is shown in figure 13.

As it can be seen in figure 13, at the beginning stages of the test, the shear stress components on all of micro-planes are zero and normal components are increased linearly.

During decrease of axial compression and creation of shear forces consequently, the shear stress components are appeared on the inclined micro-planes number 1 to 8 while at the same time the normal components are developed on the whole planes (exception of plane 11 on which the normal stress is kept constant according to the test results) and got to its maximum values when the peak axial stress is reached. Therefore, the predicted behavior of micro-planes under the CTE test is perfectly logical.
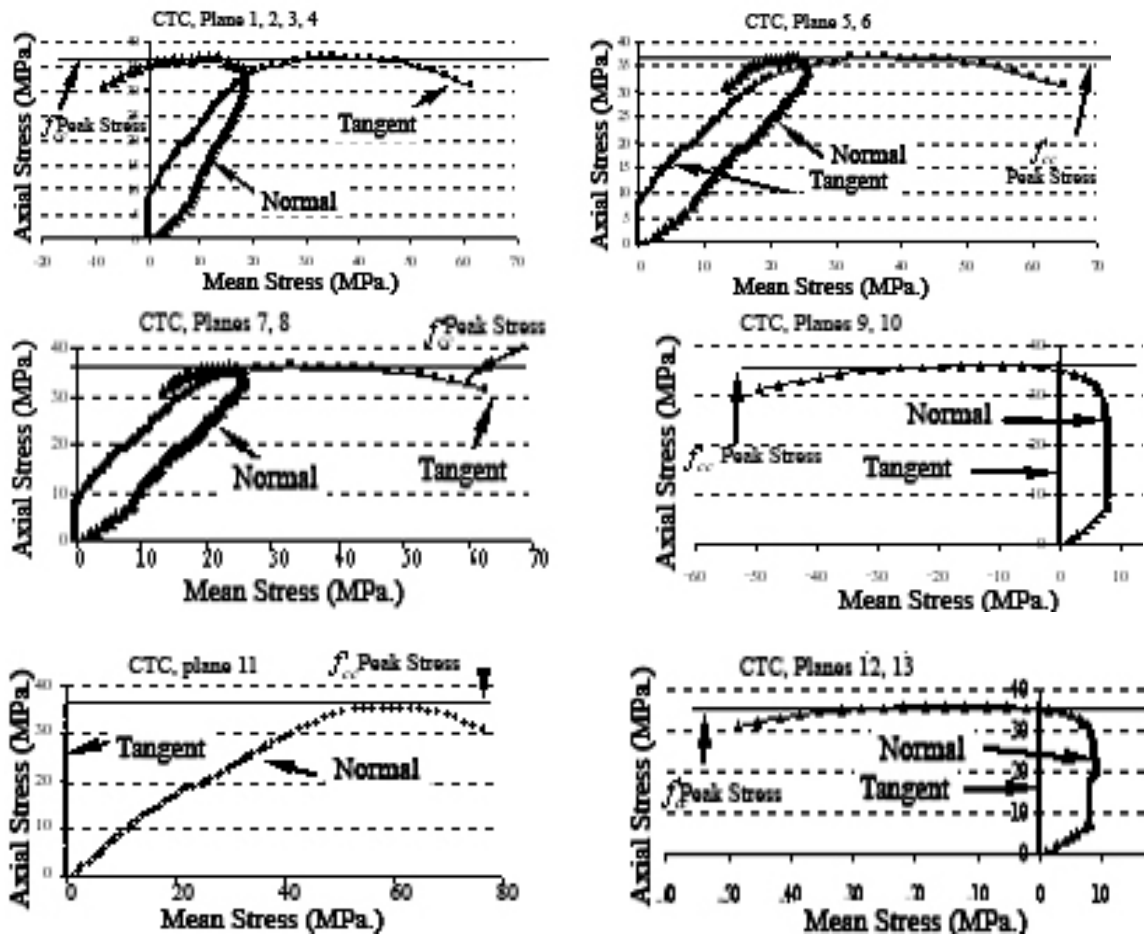
**306**

**Fig.10** Variation of micro-stress component values during Conventional Triaxial Compression (CTC) test
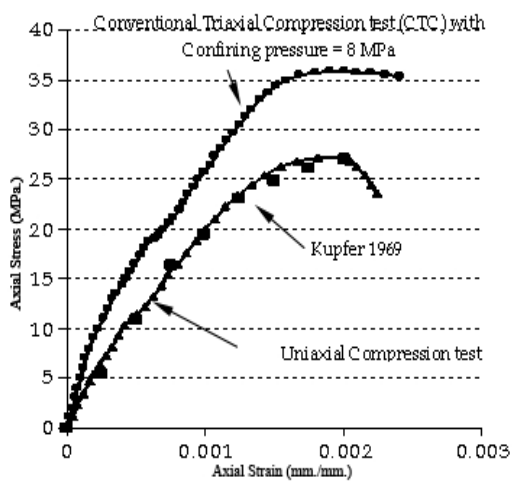


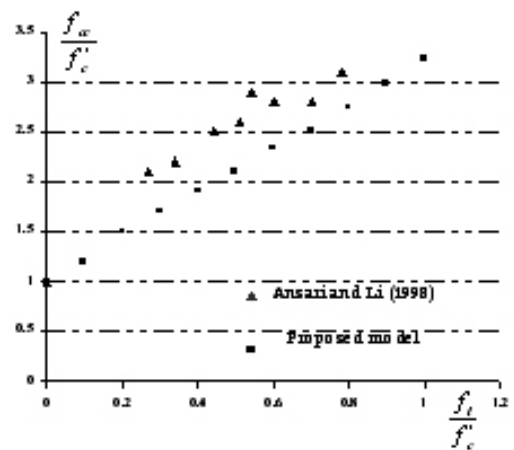**Fig.11** Comparison of axial stress-strain curves of concrete in UC and CTC tests



**Fig.12** Different triaxial compression strengths $f_{cc}$ obtained with respect to different lateral confining pressures $f_t$
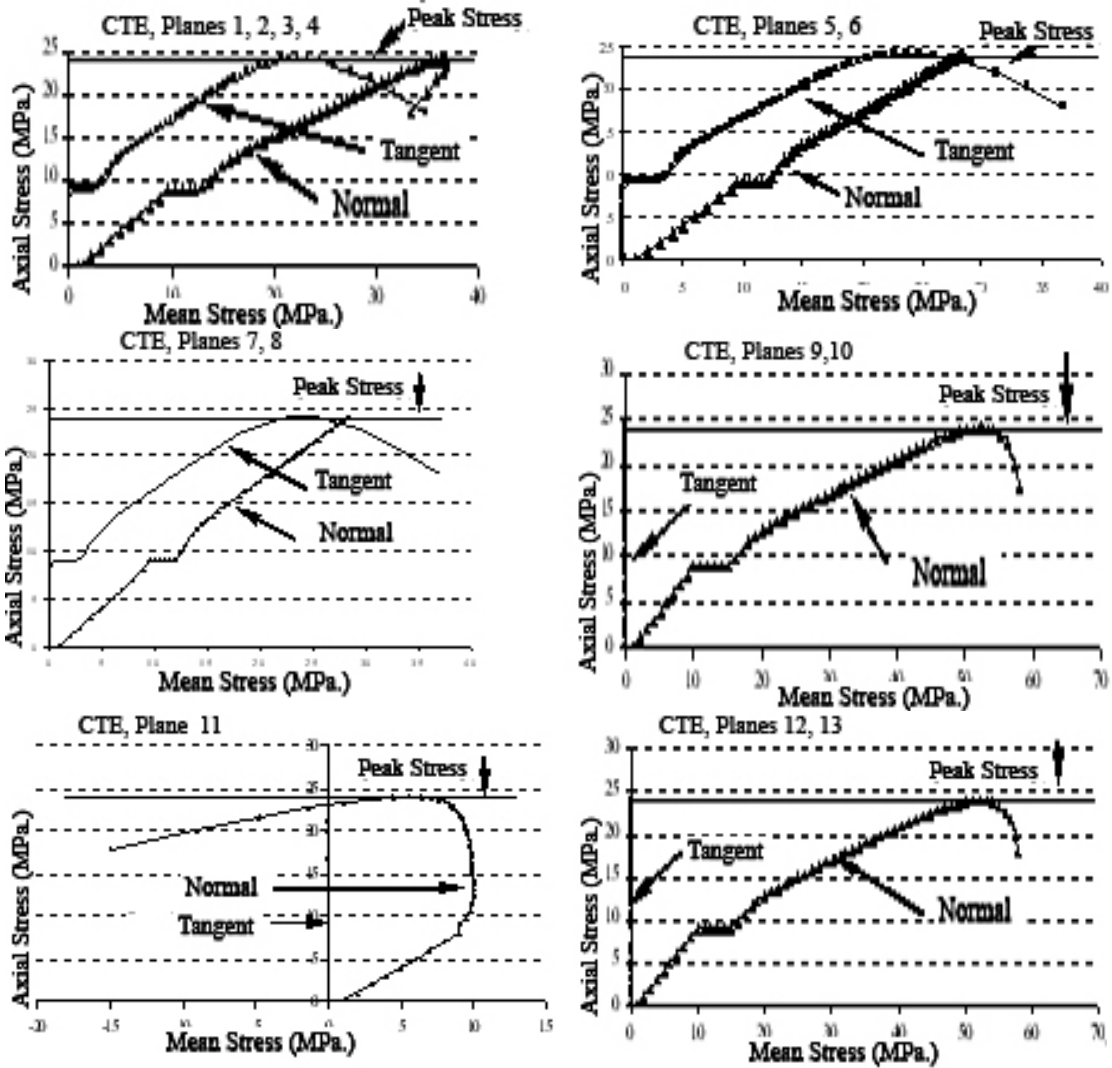
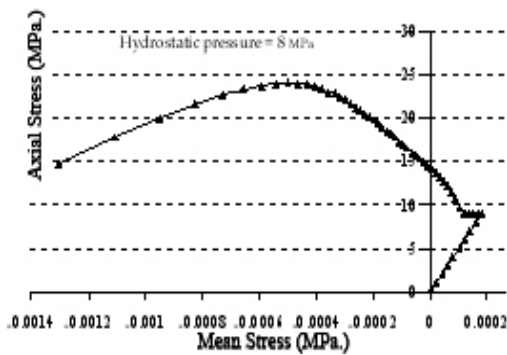**Fig.13** Variation of micro-stress component values during Conventional Triaxial Extension (CTE) test



**Fig.14** Behavior of cylindrical concrete specimen under Conventional Triaxial Extension (CTE) test obtained with proposed micro-plane damage model
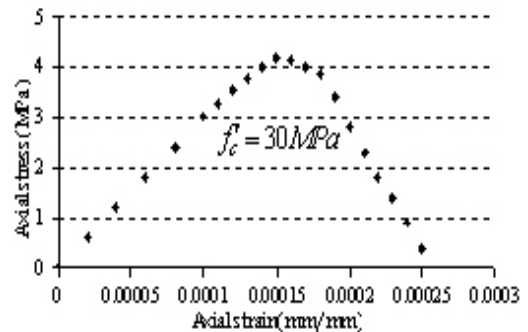


**Fig.15** Behavior of cylindrical concrete specimen under uniaxial tension test obtained with proposed micro-plane damage model
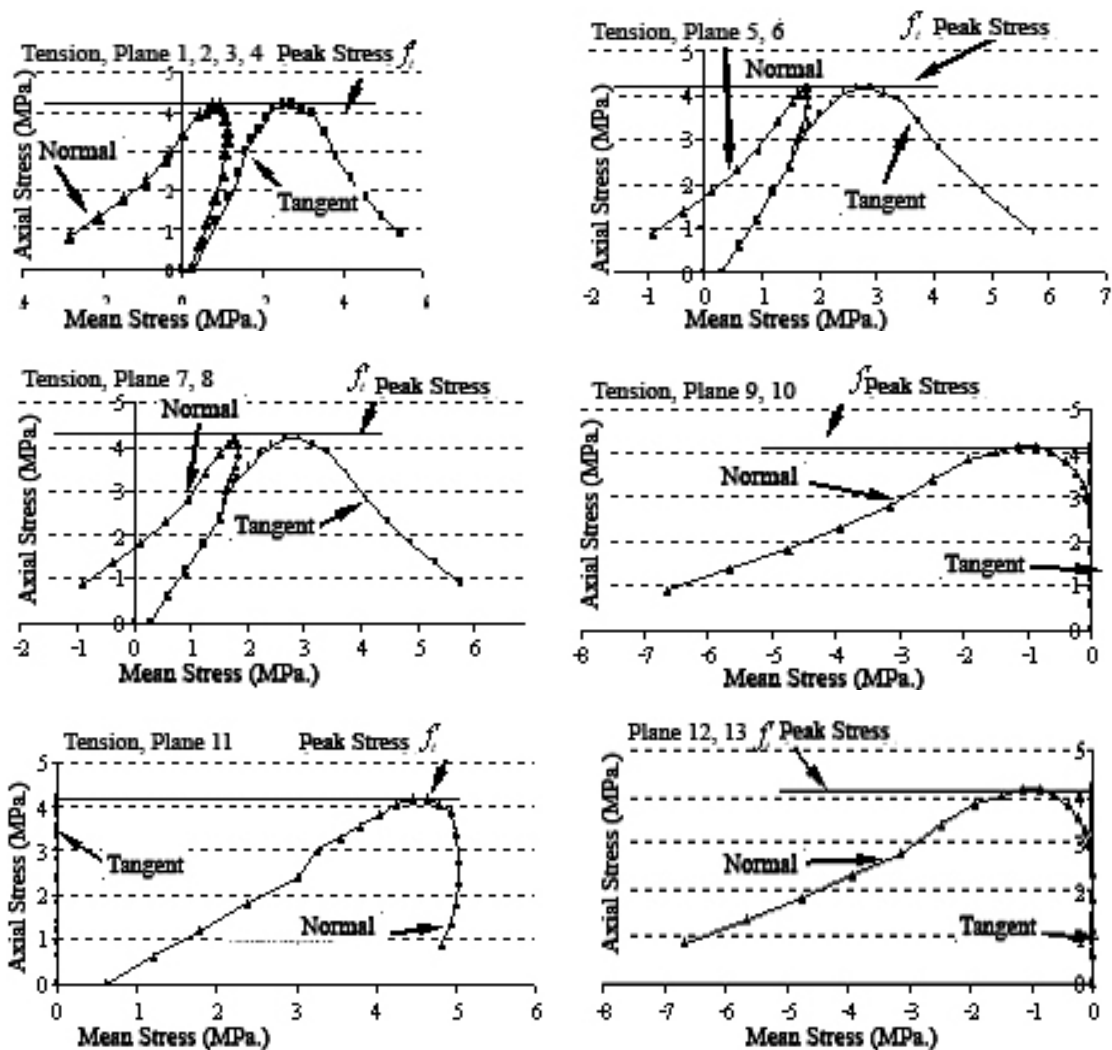
**Fig.16** Variation of micro-stress component values during Uniaxial Tension (UT) test

**Uniaxial Tension (UT) test**

The stress-strain response of the concrete cylindrical specimen under axial tension load is depicted in figure 15.

Revenue mechanism of micro-planes under the action of UT test is represented in figure 16. As it is expected, the damage on the inclined planes 1 to 8 is due to compromise of tensile and shears action. If we compare this picture with figure 7, the combination of tension and shear forces will produce damages much more quickly than

compression and shear forces.

**Hydrostatic Tension (HT) test**

In figure 17 the proposed model prediction under HT test is depicted. As it is waiting for, the load capacity of the sample under the hydrostatic tension is greater than the same value in the uniaxial tension test because in the uniaxial tension test the cause of the damage is the compromise of tension and shear stress while in the hydrostatic tension test, pure tensile stress acting on the planes.

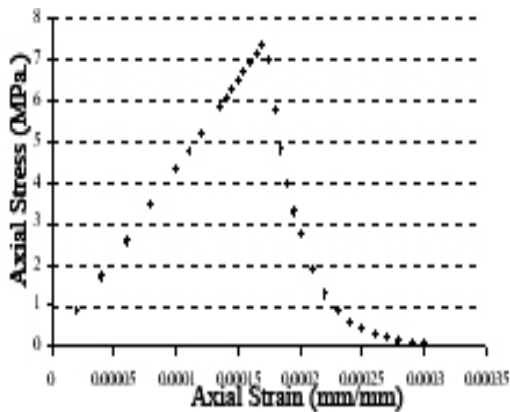The prediction of the proposed micro-planes

**Fig.17** Behavior of cylindrical concrete specimen under Hydrostatic Tension test obtained with proposed micro-plane damage model
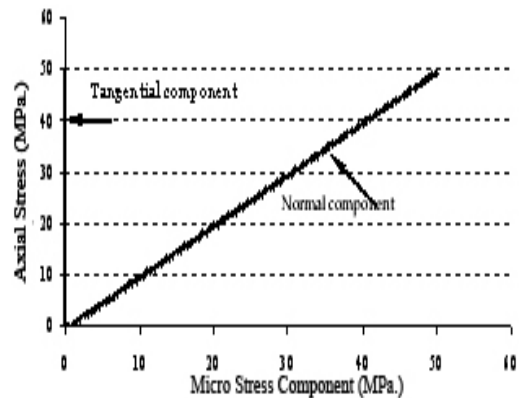


**Fig.20** Variation of micro-stress component values acting on the micro-planes number 1 to 13 during Hydrostatic Compression (HC) test
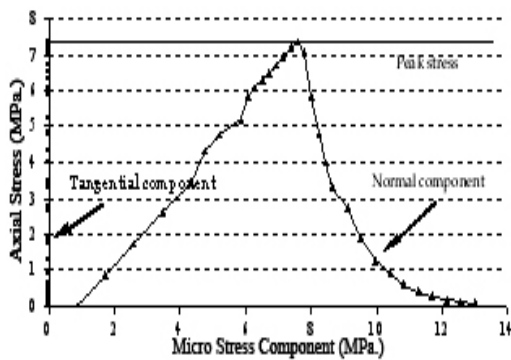


**Fig.18** Variation of micro-stress component values acting on the micro-planes number 1 to 13 during Hydrostatic Tension (HT) test
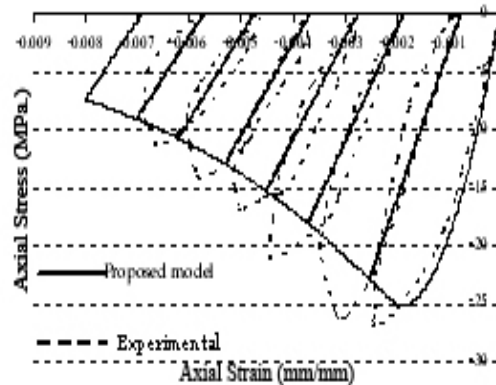


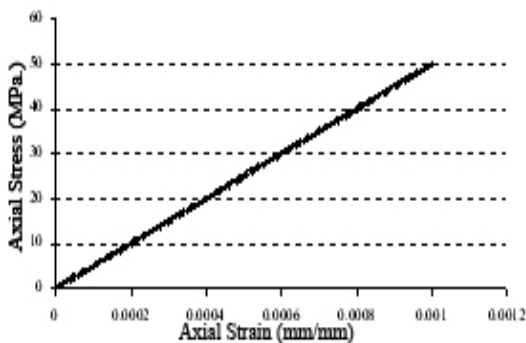**Fig.21** cyclic compression test simulation



**Fig.19** Behavior of cylindrical concrete specimen under Hydrostatic Compression test obtained with proposed micro-plane damage model
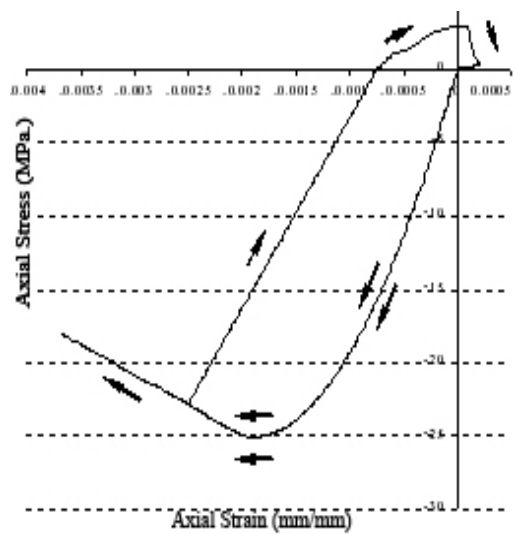


**Fig.22** complete cyclic test simulation

for the HT test is shown in the figure 18. As it can be observed the behavior of all the micro-planes under this loading is the same. The reson is that in the hydrostatic loading, the same condition of stress distributions are imposed around the physical point and therefore the anisotropy could not to be appeared. Furthermore as it is anticipated, there is no any shear stress on the planes.

### Hydrostatic Compression (HC) test

The expected response of concrete cylindrical specimen under hydrostatic compressive loading, associated with the increase of bearing capacity unlimitedly. Simulation of this response under the HC test is presented in figure 19, 20. As in the case of hydrostatic tension test, the behavior of the whole planes under the HC test is the same.

### Cyclic loading

Generally, the most damage models fail to reproduce the irreversible strains and the slopes of the curve in unloading and reloading regions.

To overcome this problem, often the plasticity and damage models are combined. In figure 21, the predicted response of the model under cyclic compression test is compared with the experimental results of B.P. Sinha, K.H. Gerstle and L.G. Tulin (1964). Obviously, there is a good agreement between the analytical and experimental data. Also, predicted behavior of concrete under complete cyclic loading is shown in figure 22.

## 5.Conclusion

A constitutive damage model for the mechanical behavior of concrete under any arbitrary loading developed using the composition of a new theoretical micro-plane

framework.

The proposed model is a micro-planes based, upon a certain micro-plane based stress/strains, satisfying both equilibrium and compatibility conditions. This characteristic of the model is called double constraint.

A new damage formulation has been employed into the micro-plane model. This damage formulation has been built on the basis of five fundamental force conditions that essentially can be occurred on each micro-plane. Consequently, any arbitrary change of six strain/stress components led to a combination of five introduced on plane coditions. Therefore, the proposed model is capable of predicting the concrete behavior under any arbitrary strain/stress path. These five force conditions are as:

- hydrostatic compression,
- hydrostatic extension,
- pure shear,
- shear + compression,
- shear + extension.

The five damage evolution are function of equivalent strain were formulated for any of the five stated conditions. The equivalent strain for the two first conditions are defined as limitation in volumetric strain and for the others is the superimposed of projections of deviatoric strain tensor on the corresponding micro-plane. These damage functions are constructed with respect to the experimental evidences on the concrete specimens under compressive and tensile loading conditions.

The proposed model has excellent features such as prefailure strain distribution inside material led to final failure mechanism, capability of seeing induced/inherent anisotropy and also any fabric effects on material behavior. However the basis of its

formulation is simple, logical and has some physical insights that make it convenient to perceive.

## References

[1] Batdorf, S.B., Budiansky, B. "A mathematical theory of plasticity based on the concept of slip.", Technical Note 1871, National Advisory Committee for Aeronautics., 1949.

[2] Ramm, E., G. A. D'Addetta, and M. Leukart."From microscopic to macroscopic modeling of geomaterials". European Congress on Computational Methods in Applied Sciences and Engineering, 2004.

[3] Bazant, Z.P., P.G. Gambarova. "Crack shear in concrete: Crack band micro plane model." J. Struct. Eng., ASCE, 110, pp.2015-2036, 1984.

[4] Bazant, Z., B.Oh. "Micro plane model for progressive fracture of concrete and rock." J. E. Mech., 111, pp.559-582, 1985.

[5] Bazant, Z., P. Prat. "Micro plane model for brittle plastic material: Part I & II. "J. E. Mech., 114, pp.1672-1702, 1988. Carol, I., Z. Bazant. "Damage and plasticity in micro plane theory." Int. J. Solids & Structures., 34, pp.3807-3835. 1997.

[6] Carol, I., Z. P. Bazant and P. Prat. "New explicit microplane model for concrete: Theoritical aspects and numerical implementation." Int. J. Solids & Structures, 29, 1173-1191, 1992.

[7] Carol, I., M. Jirasek and Z. P. Bazant.

"A thermodynamically consistent approach to micro plane theory. Part I: Free energy and consistent micro plane stresses." Int. J. Solids & Structures, 38, 2921-2931, 2001.

[8] Kuhl, E., E. Ramm and R. de Borst. "An anisotropic gradient damage model for quasi-brittle materials.", Comp. Meth. Appl. Mech. Eng., 183, 87-103, 2000.

[9] Kuhl, E. and E. Ramm. "Micro plane modeling of cohesive frictional materials. ", Eur. J. Mech." A/Solids, 19, S121-S143, 2000.

[10] Simo, J. and J. Ju. "Strain and stress based continuum damage models: Part I-Formulation, Part II-Computational aspects.", Int. J. Solids and Structures 23, pp.821-869, 1987.

[11] Bazant, Z. P., Adley, M. D., Carol, I., Jirasek, M., Akers, S.A., Rohani, B., Cargile, J.D., Caner, F.C. "Large-strain generalization of micro plane constitutive model for concrete and application." ASCE, J. Engrg. Mech. 126(9), 971-980, 2000a.

[12] Bazant, Z. P., Caner, F. C., Carol, I., Adley, M.D., Akers, S.A. "Micro plane model M4 for concrete: I. Formulation with work-conjugate deviatoric stress. "ASCE, J. Engrg. Mech. 126(9), 944-953, 2000b.

[13] Bazant, Z. P., Caner, F. C. "Micro plane M4 for concrete: II. Algorithm and calibration. ASCE, J. Engrg. Mech. 126, 954-961, 2000.

[14] Ozbolt, J., Li, Y., Kozar, I. "Micro plane model for concrete with relaxed

kinematic constraint.", Int. J. Solids Struct. 38, 2683-2711, 2001.

[15] Pijaudier-Cabot, G., Z. P. Bazant. "Non local damage theory.", J. Engrg. Mech. ASCE, 113, 1512-1533, 1987.

[16] Mazars, J. "A description of micro and macro scale damage of concrete structures." , J. Engrg. Fracture Mech., 25, pp. 729-737, 1986.

[17] Meschke, G., Lackner, R., Mang, H. "An anisotropic elastoplastic-damage

model for plane concrete.", Int. J. Numerical Methods in Engrg., 42, pp. 703-727, 1998.

[18] Yazdani, S. and Schreyer, H.L. "An anisotropic damage model with dilatation for concrete.", Mechanics of Materials 7, pp. 231-244, 1988.

[19] Lubarda, V. A. and Krajcinovic, D."Damage tensor and the crack density distribution.", Int. J. Solids Structures, Vol. 30, No. 20, pp. 2859-2877, 1993.